JACS
JOURNAL OF THE AMERICAN CHEMICAL SOCIETY
Communication
pubs.acs.org/JACS

Synthesis of Large Dendrimers with the Dimensions of Small Viruses

Jongdoo Lim,[†] Mauri Kostiainen,[‡] Jan Maly,[§] Viviana C. P. da Costa,[†] Onofrio Annunziata,[†] Giovanni M. Pavan,[∥] and Eric E. Simanek*[,†]

[†]Department of Chemistry, Texas Christian University, Fort Worth, Texas 76129, United States
[‡]Department of Applied Physics, Aalto University, Helsinki, Finland
[§]Department of Biology, J. E. Purkyně University, Ústí nad Labem, Czech Republic
[∥]Department of Innovative Technologies, University of Applied Science of Southern Switzerland, Manno 6928, Switzerland

Supporting Information

ABSTRACT: The dendrimer chemistry reported offers a route to synthetic target molecules with spherical shape, well-defined surface chemistries, and dimensions that match the size of virus particles. The largest target, a generation-13 dendrimer comprising triazines linked by diamines, is stable across ranges of concentration, pH, temperature, solvent polarity and in the presence of additives. This dendrimer theoretically presents 16 384 surface groups and has a molecular weight exceeding 8.4 MDa. Transmission electron and atomic force microscopies, dynamic light scattering, and computations reveal a diameter of ∼30 nm. The target was synthesized through an iterative divergent approach using a monochlorotriazine macromonomer providing two generations of growth per synthetic cycle. Fidelity in the synthesis is supported by evidence from NMR spectroscopy, mass spectrometry, and high-pressure liquid chromatography.

Viruses—with diameters ranging from 20 to 400 nm—occupy a length scale that represents the heart of all that is *nano*.[1] The lower bounds of this length scale are a convergent point for both top-down and bottom-up synthesis. Existing organic building blocks providing access to this size regime derive from all disciplines, including chemistry, molecular biology, and virology, and include micelles, liposomes, and viral capsids, respectively. These materials rely on self-assembly. Self-assembly reduces the burden of synthesis, but typically at the cost of stability, as reflected in sensitivity to concentration, pH, temperature, solvents, and additives such as denaturants and detergents. Covalent synthesis offers an alternative to self-assembly that provides significant opportunities for compositional control. Virus-sized, covalent organic molecules have remained elusive targets.

First described by Tomalia,[2] Newkome,[3] and Vögtle[4] in the late 1970s and early 1980s, dendrimers are highly branched, globular macromolecules that present multiple surface groups on the periphery. These architectures have been the focus of experimental and theoretical investigations in areas including materials science and medicinal chemistry.[5] While a myriad of platforms have been described, a handful have been the focus of intense scrutiny because of their ease of synthesis and/or commercial availability. These materials include the polylysines introduced by Denkewalter,[6] the poly(propylene imine) (PPI) dendrimers of Vögtle[4] and Meijer,[7] the polyamidoamine (PAMAM) dendrimers of Tomalia,[2] the polyaryl ethers of Fréchet,[8] the polyesters advanced by Gillies and Fréchet,[9] and the phosphorus-containing dendrimers of Majoral and Caminade.[10] Still, the synthesis of large-generation dendrimers is rare. Reports of large dendrimers include PAMAM[11] and phosphorus-containing dendrimers,[10,12] both of which are commercially available up to generation 10. Phosphorus-based dendrimers have long occupied the benchmark for large molecules, but at generation 12 they encounter a solubility challenge that precludes additional pursuits.[12b] At these generations, however, both this platform and PAMAM dendrimers reach diameters of only 14−15 nm. As such, these materials populate the length scale of proteins but fall short of the length scales of viruses.

For many years, we have been interested in triazine dendrimers.[13] Synthetically, these materials are derived from cyanuric chloride and diamines that can be elaborated into dendrimer cores and monomers. As a platform, this class of dendrimers offers a number of benefits, including (i) low cost of reagents, (ii) compositional diversity stemming from the wealth of available diamines and the stepwise substitution of the triazine nucleus, (iii) ease of large-scale synthesis, (iv) stability in highly acidic (pH 0) or basic (pH 14) solutions, and (v) long shelf life. These materials can be prepared using either convergent or divergent approaches, although the only latter provides access to large molecules.

To reach the target generation-13 dendrimer, **G13**, the synthesis started with a generation-1 amine core, **G1**, that was reacted with macromonomer **M** (Figure 1). Reaction of **G1** with **M** provides the protected **G3** dendrimer. Upon deprotection, the process is repeated iteratively. By design, macromonomer **M** had a single reactive site, a monochlorotriazine, which precludes the formation of covalent dimers, thereby limiting side products. Previously, in order to synthesize large dendrimers, we employed two different diamines as linkers: piperazine and an oligoether diamine.[13c] This synthetic approach was successful up to generation 9, but poor solubility was encountered at generation 11. The former diamine, piperazine, provides a more reactive, rigid linking group without hydrogen-bond donors. The latter sacrifices

Received: January 14, 2013
Published: February 12, 2013

dx.doi.org/10.1021/ja400432e | J. Am. Chem. Soc. 2013, 135, 4660−4663

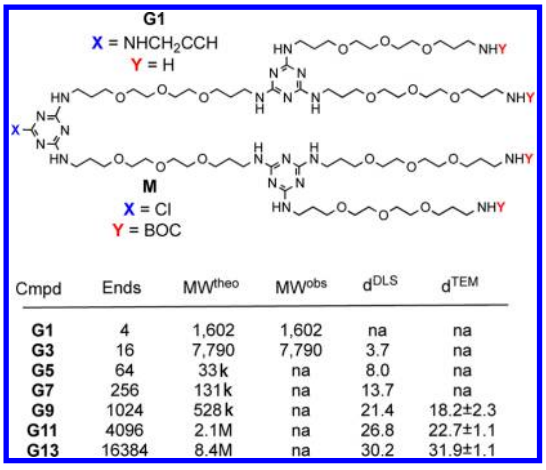

Cmpd	Ends	MW^{theo}	MW^{obs}	d^{DLS}	d^{TEM}
G1	4	1,602	1,602	na	na
G3	16	7,790	7,790	3.7	na
G5	64	33k	na	8.0	na
G7	256	131k	na	13.7	na
G9	1024	528k	na	21.4	18.2±2.3
G11	4096	2.1M	na	26.8	22.7±1.1
G13	16384	8.4M	na	30.2	31.9±1.1

Figure 1. Structures of the **G1** dendrimer with an alkyne core and the monomer **M** that is reacted to install two additional generations per iteration. "Cmpd" lists the intermediate dendrimer compounds accessed in route to **G13**. The number of end groups ("Ends"), the theoretical ("MW^{theo}") and observed ("MW^{obs}") molecular weights (in Da, as determined by ESI−TOF MS), and the diameters (in nm) obtained by DLS ("d^{DLS}") and TEM ("d^{TEM}") are indicated. The d^{TEM} data include the stain in the measurement and provide an upper limit on the size.

reactivity for flexibility and length and introduces hydrogen-bond donors and acceptors. Here, only the latter flexible diamine was adopted. Dendrimers comprising this diamine showed excellent solubility (>100 mg/mL) at all generations explored. The protected dendrimers are readily soluble in organic solvents. The amine-terminated dendrimers show good solubility in both water and organic solvents.

Target **G13** is the largest dendrimer reported to date with 13 branching points (generations) between the core and the periphery (Figure 1). This target theoretically presents 16 384 amine groups on the surface and has a molecular weight (MW) exceeding 8.4 MDa. However, because of the size of **G13**, the extent to which the actual target(s) of this synthesis represent the idealized structure is unknown. Evidence for success is derived from multiple techniques, including the behavior of smaller-generation intermediates as well as the characterization of the final product. That is, the iterative synthesis revealed trends that matched expectations with regard to both differences in polarity of the protected and deprotected materials and the appearance and disappearance of characteristic lines derived from the peripheral groups in the ^{1}H NMR spectra (Figure 2a). Specifically, removing the *tert*-butoxycarbonyl (BOC) protecting group led to a change in the chemical shift of the vicinal $-CH_2-$ group from 3.2 to 2.75 ppm. While the spectra suggest a clean reaction, confidence in this interpretation is compromised by the limits of detection afforded by ^{1}H NMR spectroscopy. In view of the large number of protons in the final product (737 240 in theory), ^{1}H NMR spectroscopy cannot provide evidence of *complete* success in conversion at the final product stage or even for intermediates beyond **G3** because of inherent limits in the signal-to-noise ratio.

High-pressure liquid chromatography (HPLC) showed that larger-generation materials elute later than smaller-generation ones (Figure 2b). On the basis of the amount of readily discerned impurities in the traces, we can assign the purity of the **G13** target and other smaller-generation intermediates to be ∼95%. This purity label reflects purity in size and not atomic

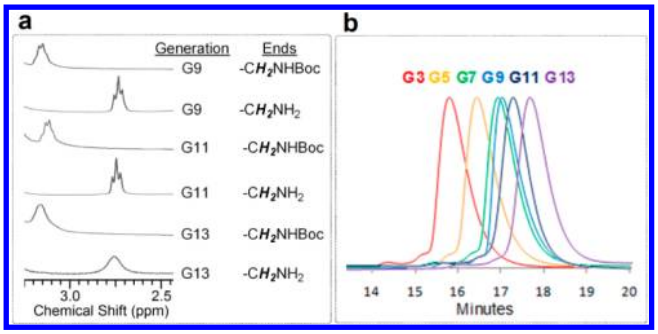

Figure 2. (a) ^{1}H NMR spectra of the large-generation dendrimers (**G9**−**G13**) in the fingerprint region for monitoring the iterative addition of **M** and deprotection. The vicinal proton signals of the NHBoc groups appear at 3.2 ppm, while the vicinal proton signals of NH_2 groups appear at 2.75 ppm. (b) HPLC traces for **G3**−**G13**.

composition of the theoretical structure depicted. We infer that these impurities are lower-MW species that may arise from incomplete deprotection or incomplete reactions of **M** with the deprotected dendrimer.

The most compelling evidence for success in the preparation of virus-sized particles was provided by cryogenic transmission electron microscopy (cryo-TEM). Figure 3 shows cryo-TEM

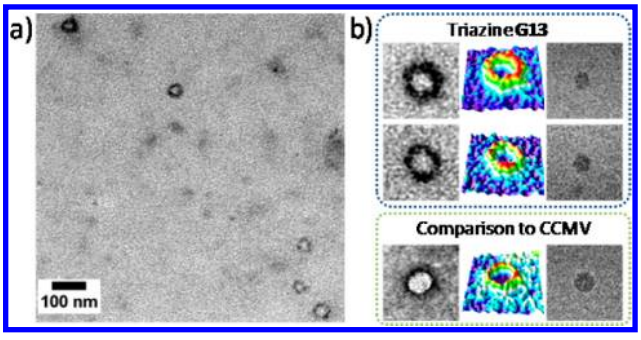

Figure 3. (a) TEM image of **G13** (sample dried and negatively stained with uranyl acetate). (b) Close-up view of the **G13** dendrimer and comparison to CCMV: (left) dry samples prepared by negative staining; (middle) colored 3D intensity profiles; (right) samples derived from vitrified aqueous solutions. Image sizes: 100 nm × 100 nm.

images of **G13** and cowpea chlorotic mottle virus (CCMV), an icosahedral RNA plant virus. X-ray crystallography and TEM revealed that the virus has a diameter of ∼28 nm. The microscopy images show similar sizes and shapes for the virus and **G13**. Both appear spherical when imaged either as dried samples stained to provide high contrast or as vitrified aqueous solutions. Because the staining is imperfect, a range of sizes rather than a single value is obtained. If the stain does not penetrate the dendrimer significantly (the standard assumption), the diameter of **G13** is 24.4 ± 2.3 nm. If the dye layer is included with the belief that partial penetration occurs because of the nature of the periphery, the dimension increases to 31.9 ± 1.1 nm. Unstained samples derived from vitrified solutions provided a diameter of 25.2 ± 2.3 nm, although this may slightly underrepresent the size because the image contrast at the edges of the **G13** particle is low.

Atomic force microscopy (AFM) corroborated the measurements of size and shape and suggested a hydration-state-dependent size. Figure 4 shows the AFM analysis of **G13** on atomically flat hydrophilic mica in water. The average height of

dx.doi.org/10.1021/ja400432e | J. Am. Chem. Soc. 2013, 135, 4660−4663

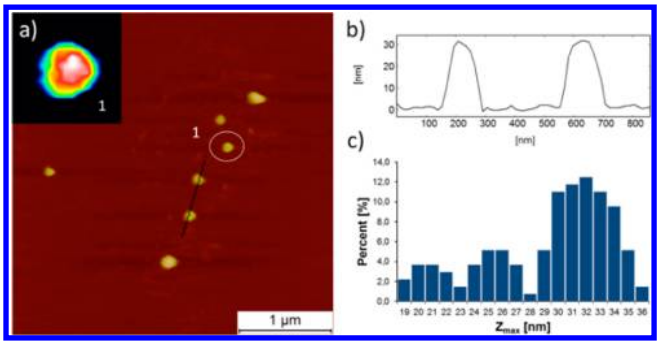

Figure 4. (a) AFM image of **G13** in water on a mica surface. Inset: close-up view (230 nm × 230 nm) of the circled **G13** dendrimer. (b) Cross-section profiles of two dendrimers (average of results for three scan lines). (c) Histogram showing the presence of two subpopulations of smaller particles in addition to **G13**.

G13 (Z_{max}), which corresponds to the dendrimer diameter assuming the ideal spherical shape, was 31.5 ± 1.9 nm. AFM analysis of dry samples suggested that the dendrimers collapse significantly in the Z dimension [Z_{max} = 9.8 ± 1.9 nm; see the Supporting Information (SI)]. This collapse suggests a high degree of hydration of the internal void space of dendrimer, or at least a higher sensitivity to the force at the AFM tip when the dendrimers are dehydrated. The results are similar to those observed by Haag with hydrogels that collapsed from ∼100 to ∼20 nm on drying.[14] The AFM size distribution also provides insights into the dispersity of the samples. The histogram in Figure 4c shows evidence for the presence of two smaller materials (∼20 and ∼25 nm diameter) along with **G13**. Representing almost 35% of the sample, these entities appear to be discrete populations of macromolecules and may correspond to materials with sizes similar to those of **G7** and **G9**/**G11**, as suggested by the HPLC traces. Their appearance is consistent with failures of purification using conventional chromatographic methods and incomplete reactions throughout the synthesis. Clearly, room for improvement exists, but this has not proven trivial to date. Filtration during sample preparation and aggregation of **G13** appeared to enrich the populations of smaller particles. Accordingly, the amount of smaller particles is likely to be closer to the HPLC-based estimates of ∼5% rather than the AFM-based estimates of ∼35%. The HPLC traces suggest that these impurities are elaborated throughout the synthesis, perhaps as a result of failed deprotection or macromonomer addition early in the process. Their existence, however, suggests opportunities for finer control over the size of particles by manipulating the valency of the dendrimer core.

Dynamic light scattering (DLS) measurements were performed on dendrimers in aqueous salt solutions at neutral pH. With the exception of **G13**, results were obtained in phosphate-buffered saline (PBS) at pH 7.0. Aggregation of **G13** in PBS required the use of 0.01 M NaCl(aq) at pH 7. With the exception of **G3**, the distribution of light-scattering intensities was found to be bimodal. The fast-diffusion mode was related to the dendrimer size using the Stokes−Einstein equation. The extracted hydrodynamic diameters (d^{DLS}) increased with dendrimer generation in going from **G3** to **G13** (Figure 1). The slow-diffusion mode can be related to the presence of large dendrimer aggregates with diameters of 50−150 nm. As hydration contributes to d^{DLS}, the values are consistent with the ranges provided by TEM and AFM. DLS measurements performed on **G13** in the absence of NaCl yielded dendrimer diffusion coefficients that were ∼10% higher. This effect can be related to the dendrimer charge and the absence of electrostatic screening.[15]

Computational models provide additional structural insights and anchored our intuitive picture of these molecules. A fully atomistic simulation in explicit solvent was not possible for **G13**, as inclusion of explicit molecules of water would have exceeded the computational infrastructure necessary for this 1.3 million atom molecule (**G13** theoretically has the formula $C_{376812}H_{737240}N_{114682}O_{98298}$). Moreover, the use of coarse-grained simplified models for **G13** was incompatible with the linear and extremely flexible character of the monomers constituting the dendritic scaffold. The construction of the **G13** atomistic model was extremely challenging because of the high structural complexity emerging from the large number of monomer connections. Molecular dynamics (MD) simulations revealed that **G13** reaches a "hard sphere" limit (Figure 5). The

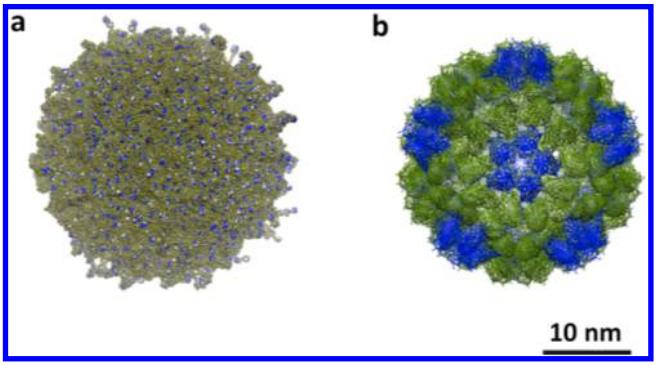

Figure 5. (a) Computational model of **G13** derived from MD simulations. Terminal amine groups are shown in blue. (b) CCMV particle colored olive and blue to illustrate the icosahedral structure.

peripheral amine groups extend not only outward but also inward by back-folding into the dendrimer, resulting in high structural density (see the radial distribution function plots in the SI). The measured radius of gyration of this molecule is R_g = 11.0−11.4 nm. This value is in good agreement with the diameters measured using DLS, as R_g and the radius of hydration (R_h) are related by the equation $R_h \approx 1.29R_g$ for spherical molecules of uniform density.[16] Accordingly, these diameters of 28.6−29.4 nm match the estimates derived from TEM and AFM.

The success in generating virus-sized materials observed here and not yet seen in PAMAM or phosphorus platforms may derive from more than just the solubility of the linking diamine. Clearly, the generation unit of the triazine dendrimers is approximately twice as long as those for the other platforms: while PAMAM relies on $-\mathbf{N}(\underline{\mathrm{R}})\mathrm{CH_2CH_2C(O)NHCH_2CH_2}-$ with seven atoms and phosphorus dendrimers rely on $-\mathbf{P}(\underline{\mathrm{R}})\mathrm{(S)O}-(p\text{-}\mathrm{C_6H_4})-\mathrm{C{=}NNH}-$ with nine atoms, the triazine platform utilizes 18 atoms per generation. In terms of the number of flexible atoms per monomer (P), de Gennes predicted the maximum size of a dendrimer with perfect branching before defects are necessitated by steric crowding of the periphery (eq 1):[17]

$$\text{limiting generation} = 2.88(\ln P + 1.5) \quad (1)$$

With P = 18, the maximum generation achieved before defects is 12.6.

dx.doi.org/10.1021/ja400432e | J. Am. Chem. Soc. 2013, 135, 4660−4663

The nature of the branching unit may be less relevant. While branching in both PAMAM and phosphorus dendrimers (indicated by R in the above formulas) occurs from a single atom (a tertiary amine N or pentavalent P, respectively, shown in bold above), both triazines and cyclophosphazene dendrimers branch from a larger rigid ring.

The covalent single-molecule nanomaterial described herein constitutes a new platform for nanosynthesis. Its viral dimensions and spherical shape are complemented by a well-defined (although not uniquely perfect) composition. Extending opportunities for functional group variation both within and on the periphery of these building materials is precedented in smaller-generation dendrimers of all classes. Polymerization chemistry offers another route to such targets. Indeed, linear and hyperbranched polymers of similar molecular weight can be achieved, although control over the shape in linear systems is not as readily guaranteed as it is with dendrimers, nor is control over the composition in hyperbranched systems.[14] Self-assembly[18] has achieved these dimensions, including Percec's dendrisomes[19] and other systems that can be subsequently cross-linked,[20] although such materials are usually more sensitive to factors including temperature, detergents, and concentration. The primary disadvantage of the present system, the burden of synthesis, has been reduced significantly by using an iterative route with a common macromonomer. Accordingly, we believe that there materials further expand the nanoperiodic table, and offer viruses.[21] These properties include (i) attachment to biological surfaces such as bacteria, cells, and bone; (ii) delivery of cargo, including nucleic acids or small molecules; and (iii) use as building blocks for hybrid materials.[22]

■ ASSOCIATED CONTENT

Supporting Information

Details of synthesis, characterization, and computation. This material is available free of charge via the Internet at http://pubs.acs.org.

■ AUTHOR INFORMATION

Corresponding Author

e.simanek@tcu.edu

Notes

The authors declare no competing financial interest.

■ ACKNOWLEDGMENTS

The authors acknowledge the following: NIH (NIGMS R01 65460, E.E.S.), the Robert A. Welch Foundation (A-0008, E.E.S.), the Academy of Finland (13137582, M.K.), the Emil Aaltonen Foundation and Aalto Starting Grant (M.K.), the Czech National COST Project (OC10053, J.M.), the Czech Science Foundation (13-06609S, J.M.), and the ACS Petroleum Research Fund (47244-G4, O.A.). This work made use of the Aalto University Nanomicroscopy Center with assistance from J. Seitsonen on cryo-TEM.

■ REFERENCES

(1) Levine, A. J. *Viruses*; Scientific American Library Series; W.H. Freeman: New York, 1992; p 240.

(2) Tomalia, D. A.; Baker, H.; Dewald, J.; Hall, M.; Kallos, G.; Martin, S.; Roeck, J.; Ryder, J.; Smith, P. *Polym. J.* **1985**, *17*, 117.

(3) Newkome, G. R.; Yao, Z. Q.; Baker, G. R.; Gupta, V. K. *J. Org. Chem.* **1985**, *50*, 2003.

(4) Buhleier, E.; Wehner, W.; Vögtle, F. *Synthesis* **1978**, 155.

(5) (a) Helms, B.; Meijer, E. W. *Science* **2006**, *313*, 929. (b) Hu, J.; Xu, T.; Cheng, Y. *Chem. Rev.* **2012**, *112*, 3856. (c) Percec, V.; Peterca, M.; Dulcey, A. E.; Imam, M. R.; Hudson, S. D.; Nummelin, S.; Adelman, P.; Heiney, P. A. *J. Am. Chem. Soc.* **2008**, *130*, 13079.

(6) Denkewalter, R. G.; Kolc, J.; Lukasavage, W. J. Macromolecular Highly Branched Homogeneous Compound Based on Lysine Units. U.S. Patent 4,289,872, 1981.

(7) de Brabander-van den Berg, E. M. M.; Meijer, E. W. *Angew. Chem., Int. Ed. Engl.* **1993**, *32*, 1308.

(8) Grayson, S. M.; Fréchet, J. M. J. *Chem. Rev.* **2001**, *101*, 3819.

(9) Gillies, E. R.; Fréchet, J. M. J. *J. Am. Chem. Soc.* **2002**, *124*, 14137.

(10) Caminade, A. M.; Majoral, J. P. *Acc. Chem. Res.* **2004**, *37*, 341.

(11) (a) Maiti, P. K.; Çağin, T.; Wang, G.; Goddard, W. A., III. *Macromolecules* **2004**, *37*, 6236. (b) Li, J.; Piehler, L. T.; Qin, D.; Baker, J. R., Jr.; Tomalia, D. A. *Langmuir* **2000**, *16*, 5613.

(12) (a) Caminade, A. M.; Laurent, R.; Majoral, J. P. *Adv. Drug Delivery Rev.* **2005**, *57*, 2130. (b) Majoral, J. P.; Caminade, A. M. *Top. Curr. Chem.* **1998**, *197*, 79.

(13) (a) Simanek, E. E.; Abdou, H.; Lalwani, S.; Lim, J.; Mintzer, M. A.; Venditto, V. J.; Vittur, B. *Proc. R. Soc. A* **2010**, *466*, 1445. (b) Lim, J.; Simanek, E. E. *Adv. Drug Delivery Rev.* **2012**, *64*, 826. (c) Lim, J.; Pavan, G. M.; Annunziata, O.; Simanek, E. E. *J. Am. Chem. Soc.* **2012**, *134*, 1942.

(14) Zhou, H.; Steinhilber, D.; Schlaad, H.; Sisson, A. L.; Haag, R. *React. Funct. Polym.* **2011**, *71*, 356.

(15) Schmitz, K. S. *An Introduction to Dynamic Light Scattering by Macromolecules*; Academic Press: San Diego, 1990; pp 205−214.

(16) Jensen, L. B.; Mortensen, K.; Pavan, G. M.; Kasimova, M. R.; Jensen, D. K.; Gadzhyeva, V.; Nielsen, H. M.; Foged, C. *Biomacromolecules* **2010**, *11*, 3571.

(17) de Gennes, P. G.; Hervet, H. *J. Phys., Lett.* **1983**, *44*, L351.

(18) Whitesides, G. M.; Mathias, J. P.; Seto, C. T. *Science* **1991**, *254*, 1312.

(19) (a) Peterca, M.; Percec, V.; Leowanawat, P.; Bertin, A. *J. Am. Chem. Soc.* **2011**, *133*, 20507. (b) Percec, V.; Wilson, D. A.; Leowanawat, P.; Wilson, C. J.; Hughes, A. D.; Kaucher, M. S.; Hammer, D. A.; Levine, D. H.; Kim, A. J.; Bates, F. S.; Davis, K. P.; Lodge, T. P.; Klein, M. L.; DeVane, R. H.; Aqad, E.; Rosen, B. M.; Argintaru, A. O.; Sienkowska, M. J.; Rissanen, K.; Nummelin, S.; Ropponen, J. *Science* **2010**, *328*, 1009.

(20) O'Reilly, R. K.; Hawker, C. J.; Wooley, K. L. *Chem. Soc. Rev.* **2006**, *35*, 1068.

(21) (a) Tomalia, D. A. *Soft Matter* **2010**, *6*, 456. (b) Tomalia, D. A. *New J. Chem.* **2012**, *36*, 264. (c) Tomalia, D. A.; Christensen, J. B.; Boas, U. *Dendrimers, Dendrons and Dendritic Polymers*; Cambridge University Press: Cambridge, U.K., 2012.

(22) Kostiainen, M. A.; Hiekkataipale, P.; Laiho, A.; Lemieux, V.; Seitsonen, J.; Ruokolainen, J.; Ceci, P. *Nat. Nanotechnol.* **2013**, *8*, 52.